Scientific Research Publishing

Applied Mathematics, 2020, 11, 650-669
https://www.scirp.org/journal/am
ISSN Online: 2152-7393
ISSN Print: 2152-7385

# Impact of Chloride Channel on Spiking Patterns of Morris-Lecar Model

**Tahmineh Azizi, Bacim Alali**

Department of Mathematics, Kansas State University, Manhattan, KS, USA
Email: tazizi@ksu.edu

**How to cite this paper:** Azizi, T. and Alali, B. (2020) Impact of Chloride Channel on Spiking Patterns of Morris-Lecar Model. *Applied Mathematics*, **11**, 650-669.
https://doi.org/10.4236/am.2020.117044

**Received:** June 25, 2020
**Accepted:** July 20, 2020
**Published:** July 23, 2020



## Abstract

In this paper, we study the complicated dynamics of general Morris-Lecar model with the impact of $Cl^-$ fluctuations on firing patterns of this neuron model. After adding $Cl^-$ channel in the original Morris-Lecar model, the dynamics of the original model such as its bifurcations of equilibrium points would be changed and they occurred at different values compared to the primary model. We discover these qualitative changes in the point of dynamical systems and neuroscience. We will conduct the co-dimension two bifurcations analysis with respect to different control parameters to explore the complicated behaviors for this new neuron model.

## Keywords

Chloride Channel, Supercritical Hopf Bifurcation, Subcritical Hopf Bifurcation, Firing Spike, Co-Dimension Two Bifurcations

## 1. Introduction

Computational neuroscience uses knowledge of biology and combines with mathematical modeling to simulate the fluctuations of neuron cells and biological physiological characteristics of them [1] [2] [3] [4]. The progress and advances in computational neuroscience could help scientists to better understand the performance of brain and neuron cells and better fight with diseases related to neuron cells such as Parkinson's and depression [5]. Due to the complexity of nerve systems, it is impossible to fully understand the various phenomena in neuroscience only using the simple linear modeling methods, since it does not meet all neuronal properties and complicated behaviors of neurons. Thus, we need to use nonlinear methods and models which catch all of the properties of neurons using different experimental data which brings biologist and specifically

neuroscientists and applied science people all together to develop appropriate models to explore all these complex dynamics of neurons [1] [5] [6] [7] [8].

The Morris-Lecar model is a two-dimensional biological neuron model which produces action potentials and neuronal fluctuations; in dynamical system point of view, oscillatory behaviors related to its ionic channels in giant barnacle muscle fibers [9] [10]. Kathleen Morris and Harold Lecar proposed this simple two-dimensional model to generate spikes in 1981 [7] [11] [12]. The Morris-Lecar model describes the electrical activities of neurons with a system of two nonlinear ordinary differential equations and includes different channels. This model reduces the four-dimensional Hodgkin-Huxley model to be a two-dimensional system of ordinary differential equations while keeping the major neuronal properties of generating action potential but through simpler mathematical model [11] [12] [13]. The general Morris-Lecar model includes three channels: a potassium channel, a leak and a calcium channel and has the following form [7]

$$\begin{cases} C_M \dfrac{\mathrm{d}V}{\mathrm{d}t} = I_{app} - g_L\left(V - E_L\right) - g_K n\left(V - E_K\right) - g_{Ca} m_\infty\left(V\right)\left(V - E_{Ca}\right) \\ \qquad\quad = I_{app} - I_{ion}\left(V, n\right), \\ \dfrac{\mathrm{d}n}{\mathrm{d}t} = \phi\left(n_\infty\left(V\right) - n\right) \big/ \tau_n\left(V\right), \end{cases}$$

where

$$m_\infty\left(V\right) = \frac{1}{2}\left[1 + \tanh\left(V - V_1\right)/V_2\right],$$

$$\tau_n\left(V\right) = 1/\cosh\left(\left(V - V_3\right)/\left(2V_4\right)\right),$$

$$n_\infty\left(V\right) = \frac{1}{2}\left[1 + \tanh\left(\left(V - V_3\right)/V_4\right)\right].$$

and

$$I_{ion}\left(V, n\right) = g_L\left(V - E_L\right) + g_K n\left(V - E_K\right) + g_{Ca} m_\infty\left(V\right)\left(V - E_{Ca}\right)$$

where $V$ demonstrates membrane potential, and $n$ the activation variable of the persistent $K^+$ current, so it is a two-dimensional vector $\left(V, n\right)$. $E_K$, $E_{Ca}$, and $E_L$ denote the Nernst equilibrium potentials. $I_{app}$ demonstrates the injected current and $I_{ion}$ the ionic current. Parameter $\phi$ is a temperature factor. $g_L$ is leak membrane conductance, $g_K$ is potassium membrane conductance and $g_{Ca}$ is calcium membrane conductance. Moreover, $C_M$ is the total membrane capacitance. Also, the voltage-sensitive steady-state activation function $m_\infty\left(V\right)$ and $n_\infty\left(V\right)$, and the time constant $\tau_n\left(V\right)$ can be measured experimentally.

## 2. Morris-Lecar Model with the Impact of $Cl^-$ Fluctuations on Firing Patterns

In this study, we will discover the dynamics of Morris-Lecar model with the impact of $Cl^-$ channel that has the following form:

$$\begin{cases} C_M \dfrac{\mathrm{d}V}{\mathrm{d}t} = I_{app} - g_L\left(V - E_L\right) - g_K n\left(V - E_K\right) - g_{Na} m_\infty\left(V\right)\left(V - E_{Na}\right) \\ \qquad\qquad - g_{exc}\left(V - E_{exc}\right) - g_{inh}\left(V - E_{Cl}\right), \\ \dfrac{\mathrm{d}n}{\mathrm{d}t} = \Phi\left(n_\infty\left(V\right) - n\right)/\tau_n\left(V\right), \end{cases} \tag{1}$$

where

$$m_\infty\left(V\right) = \frac{1}{2}\left[1 + \tanh\left(\left(V - V_1\right)/V_2\right)\right],$$

$$\tau_n\left(V\right) = 1/\cosh\left(\left(V - V_3\right)/\left(2V_4\right)\right),$$

$$n_\infty\left(V\right) = \frac{1}{2}\left[1 + \tanh\left(\left(V - V_3\right)/V_4\right)\right].$$

Here, $E_{Cl}$, $E_{exc}$, $E_L$, $E_K$, and $E_{Na}$ the Nernst equilibrium potentials. $I_{app}$ the injected current, $g_{inh}$, $g_{exc}$, $g_L$, $g_K$, $g_{Na}$, inhibitory, excitatory, leak, potassium and sodium membrane conductance, $C_M$ the total membrane capacitance. In Neuroscience point of view, we can describe the electrical properties of a neuron with the help of an Equivalent Circuit. Here, we can write the total current $I$ as the following form

$$I = C\dot{V} + I_{Na} + I_K + I_{Cl} \quad \text{Kirchhoff's Law}$$

And Then

$$C\dot{V} = I - I_{Na} - I_K - I_{Cl}$$

And also we know

$$E_K < E_{Cl} < V < E_{Na}$$

where $I_{Na}$ (inward currents) is negative and also $I_K, I_{Cl}$ are positive. Moreover, The inward currents depolarize the neuron and outward currents hyperpolarize it. Here, we have designed an Equivalent Circuit with the help of Simulink for model (1) (see **Figure 1**).

In this paper, we focus on this novel Morris-Lecar model for a certain range of parameters value which demonstrates different types of local bifurcations such as Hopf bifurcation and homoclinic bifurcation. We use rigorous analytic dynamical systems tools to study the complicated neuronal behaviors of this model such as normal form theory. We conduct bifurcation analysis with respect to different parameters to display the effect of various biological parameters on spiking dynamics of the system. Moreover, we are interested to discover the co-dimension two bifurcations such as Bautin or generalized Hopf and Bogdanov-Takens and cusp bifurcations and we present the normal form of these bifurcations.

## 3. Supercritical Hopf Bifurcation and Subcritical Hopf Bifurcation

In dynamical system point of view, for the Hopf bifurcation, a stable focus loses

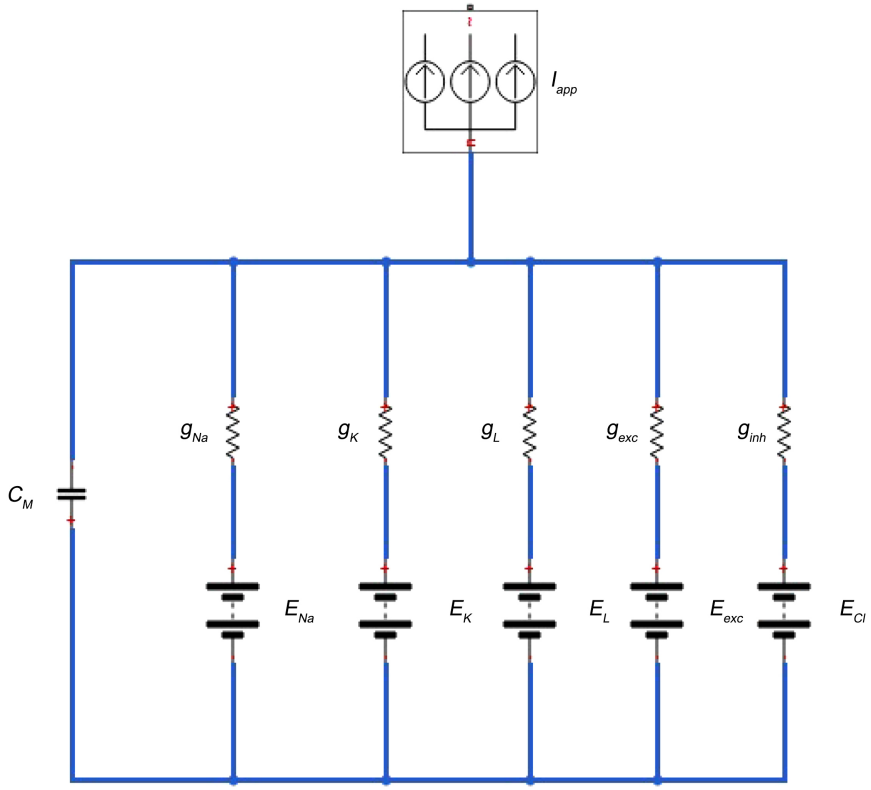


**Figure 1.** Equivalent circuit for model (1). $E_{Cl}$, $E_{exc}$, $E_L$, $E_K$, and $E_{Na}$ the Nernst equilibrium potentials. $I_{app}$ the injected current, $g_{inh}$, $g_{exc}$, $g_L$, $g_K$, $g_{Na}$, inhibitory, excitatory, leak, potassium and sodium membrane conductance, $C_M$ the total membrane capacitance.

its stability and becomes an unstable focus as we change the parameter for bifurcation, and the stable focus which is an attractor becomes a limit cycle that this limit cycle in phase space is a closed curve [1] [14] [15].

Using the parameters values corresponding to the Hopf case in **Table 1** with $\phi = 0.25$, we could get to the first Hopf bifurcation but unlike [12], this bifurcation happens for larger amount of $I_{app}$.

We have demonstrated the time series for Hopf case in **Figure 2** and **Figure 3**. As we can see the neuron for firing a spike needs a larger amount of $I_{app}$ than the model original Morris-Lecar Model in **Figure 2** of [12].

And for other values of $I_{app}$ near the Hopf bifurcation, we can see the changing in the behaviors of solutions. The neurons that show the subcritical Hopf bifurcation are resonators that exhibit bistability and the neurons that show supercritical Hopf bifurcations are resonators that exhibit monostability [1].

Continuing further, we compare the trajectories of two types of Hopf bifurcation. For model (1), we have both types of Hopf bifurcation. For supercritical Hope bifurcation that occurs for $I_{app} \approx 208$ a small limit cycle is born at the bifurcation point. This limit cycle will grow as we increase further the injected current (the amplitude of limit cycle increases with further increase of parameter). In **Figure 4** and **Figure 5**, we can easily distinguish the trajectories of these two types of Hopf bifurcation, before and after the bifurcation points.

**Table 1.** Morris-Lecar parameters [7].

| Parameter | Hopf | SNLC | Homoclinic |
|---|---|---|---|
| $\varnothing$ | 0.04 | 0.067 | 0.23 |
| $g_{Ca}$ | 4.4 | 4 | 4 |
| $V_3$ | 2 | 12 | 12 |
| $V_4$ | 30 | 17.4 | 17.4 |
| $E_{Ca}$ | 120 | 120 | 120 |
| $E_K$ | −84 | −84 | −84 |
| $E_L$ | −60 | −60 | −60 |
| $g_K$ | 8 | 8 | 8 |
| $g_L$ | 2 | 2 | 2 |
| $V_1$ | −1.2 | −1.2 | −1.2 |
| $V_2$ | 18 | 18 | 18 |
| $C_M$ | 20 | 20 | 20 |

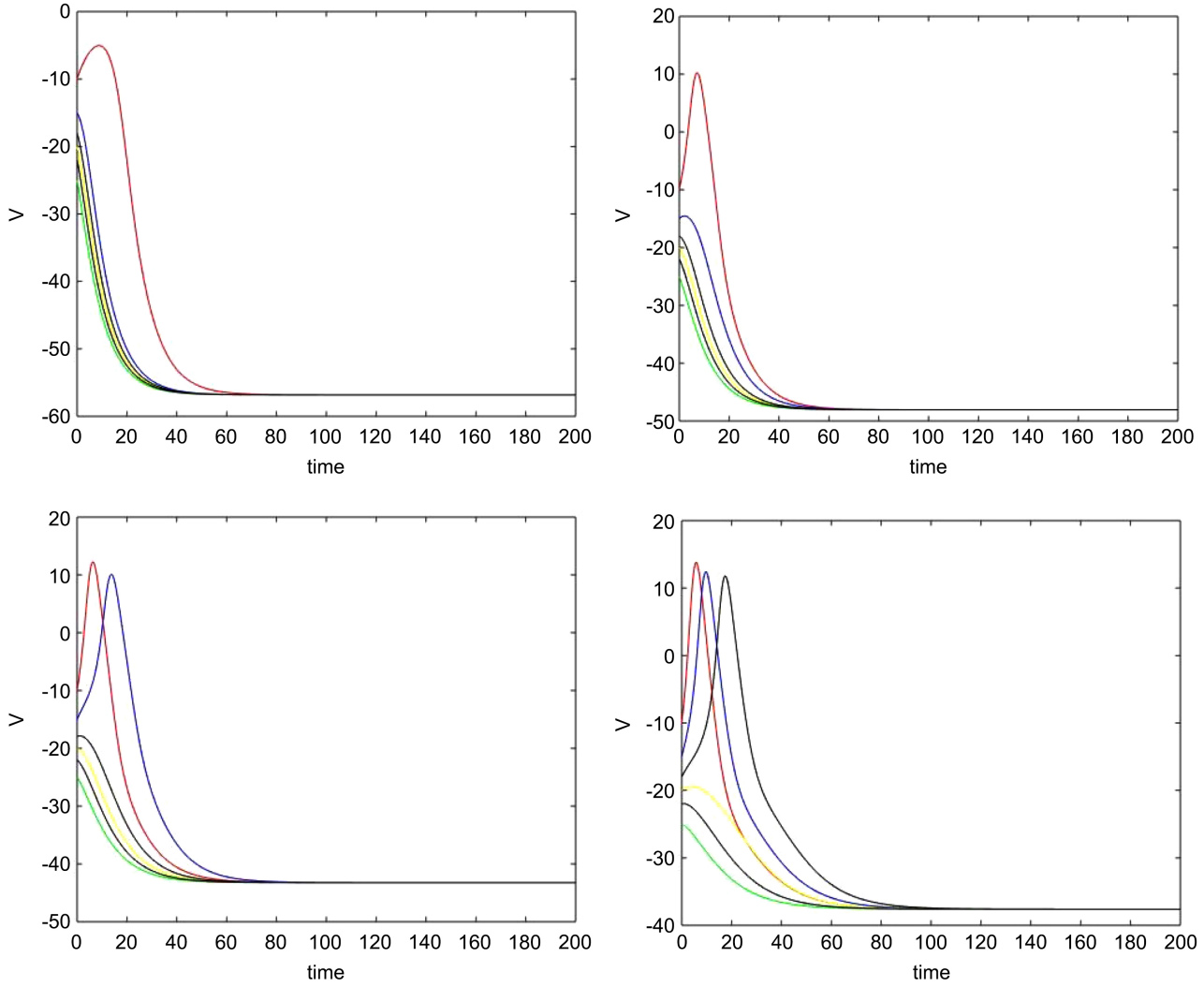


**Figure 2.** As we see the neuron needs a larger amount of injected current to spike and then after spike the solutions go back to the resting state or equilibrium state. $I_{app} = 0$ (up, left), $I_{app} = 20$ (up, right), $I_{app} = 30$ (down, left), $I_{app} = 40$ (down, right).

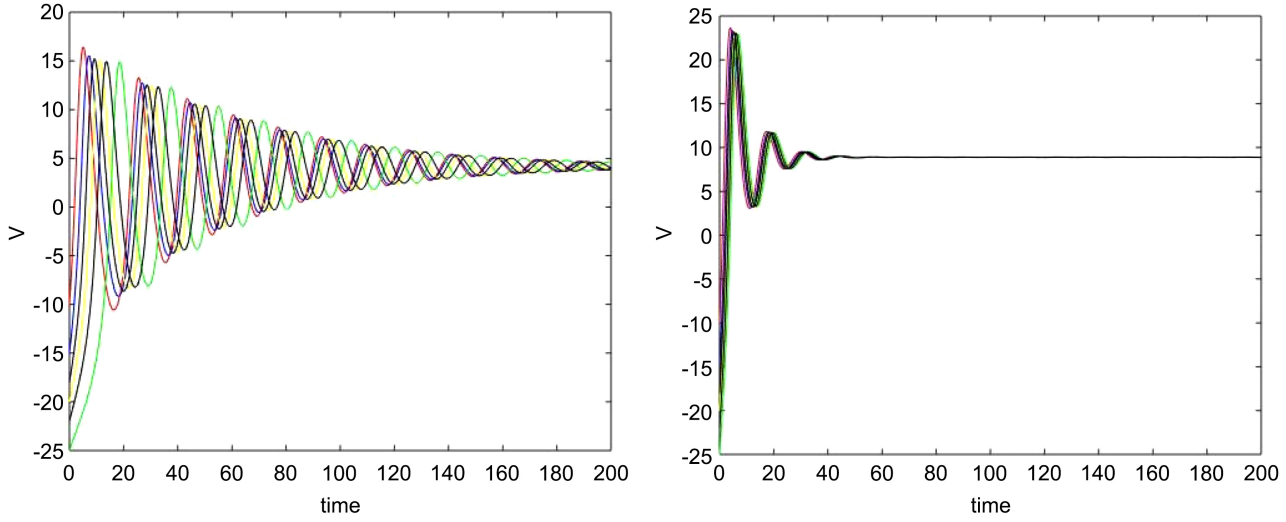


**Figure 3.** Time series of model (1) with $I_{app} = 60$ left, and $I_{app} = 137$ right.

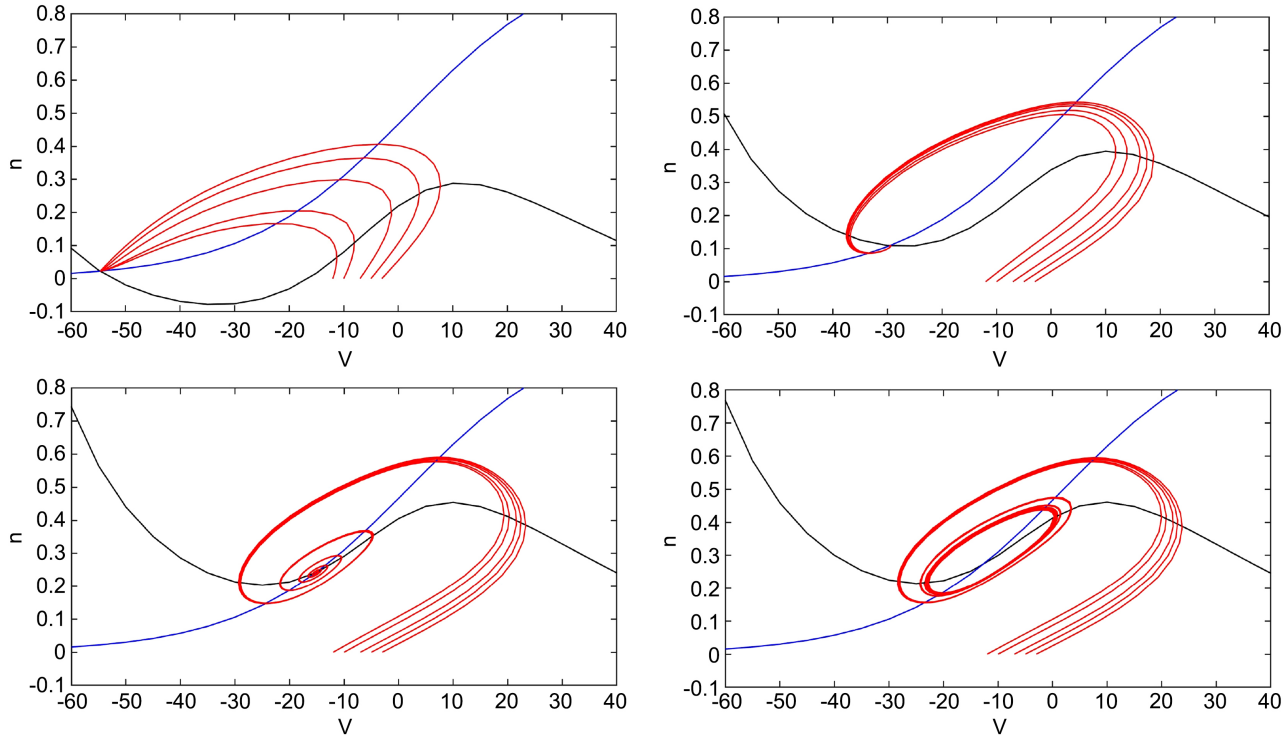


**Figure 4.** The trajectories behaviors before and after the subcritical Hopf bifurcation. Stability behaviors for $I_{app} = 10$ (up, left), Changing the behavior for $I_{app} = 90$ (up, right), Before subcritical Hopf bifurcation in $I_{app} = 135$ (down, left), After the subcritical Hopf bifurcation in $I_{app} = 140$ (down, right).

In a supercritical Hopf bifurcation, we have an equilibrium point that one limit cycle bifurcates from it. It means, for the parameter values before the parameter bifurcation, the limit cycle is degenerate and its amplitude is zero, and the amplitude extends as the parameter enhances further. But, in subcritical Hopf bifurcation, we have an unstable limit cycle around the equilibrium point, and a stable limit cycle surrounds it. This unstable limit cycle is as separatrix cycle

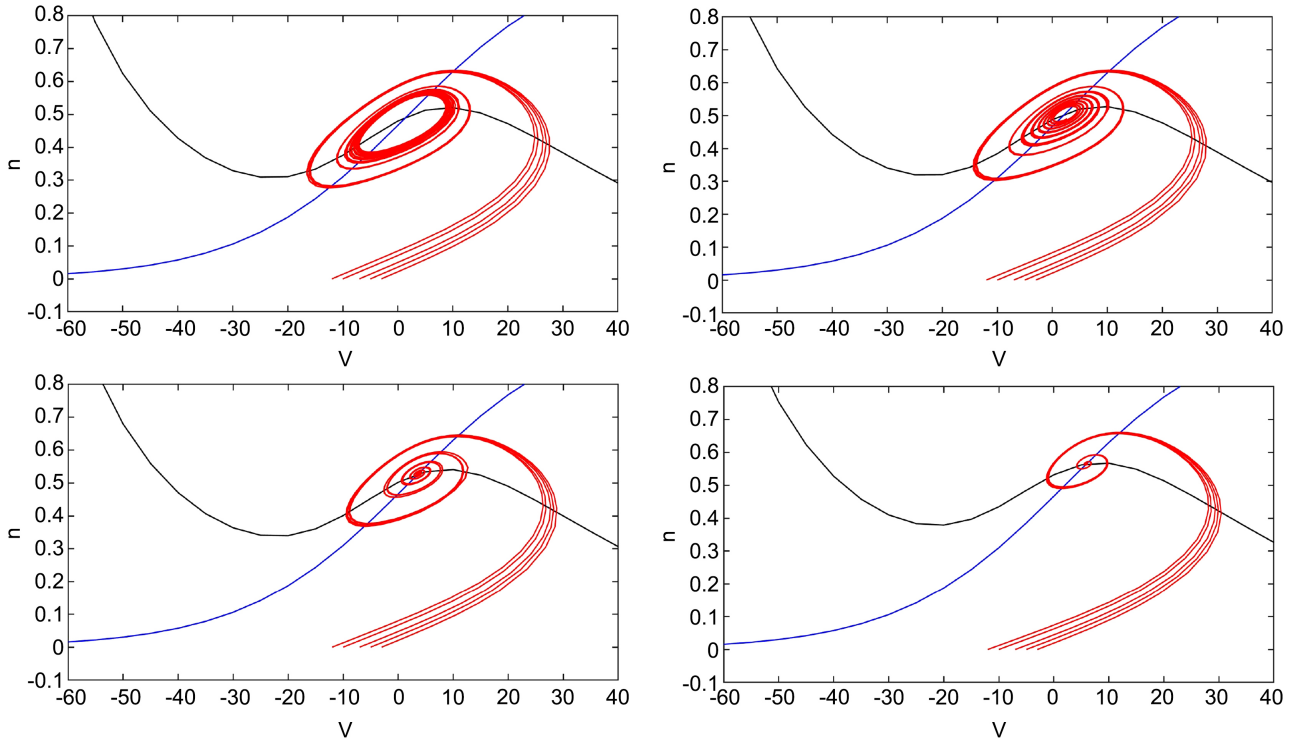


**Figure 5.** The trajectories behaviors before and after the supercritical Hopf bifurcation. Changing the type of Hopf bifurcation is clear for $I_{app}$ = 185 (up, left), $I_{app}$ = 190 (up, right), Before supercritical Hopf bifurcation in $I_{app}$ = 200 (down, left), After supercritical Hopf bifurcation in $I_{app}$ = 220 (down, right).

that separates two stable states and we could see the bistability that is not available in supercritical Hopf bifurcation and as a result only mono stability occurs in this case. The unstable limit cycle in subcritical Hopf bifurcation, degenerates to the equilibrium point, and the equilibrium points becomes unstable during this bifurcation. This type of bifurcation creates catastrophic changes in the behavior as we have suddenly changed the behavior from stable focus to oscillations with large amplitude [1] [2] [3] [4].

The bifurcation diagram for model (1) has been displayed in **Figure 6** using the parameters values from **Table 1** and with $\phi = 0.25$.

To rigorous analysis of Hopf bifurcation, as it has been demonstrated in **Figure 6**, the continuation of equilibrium points gives us two Hopf points with the following values of the normal form coefficients:

label = *H*, $x = (1.318376 \quad 0.488642 \quad 207.848139)$
First Lyapunov coefficient = −2.972401e−04

label = *H*, $x = (-12.596094 \quad 0.274268 \quad 160.995457)$
First Lyapunov coefficient = 8.624905e−05

As a result, for $I_{app} = 160.995457$ and $(V,n) = (-12.596094, 0.274268)$ we have the first Hopf point with positive First Lyapunov coefficient, and for $I_{app} = 207.848139$ and $(V,n) = (1.318376, 0.488642)$ we can see the second Hopf point with negative First Lyapunov coefficient.

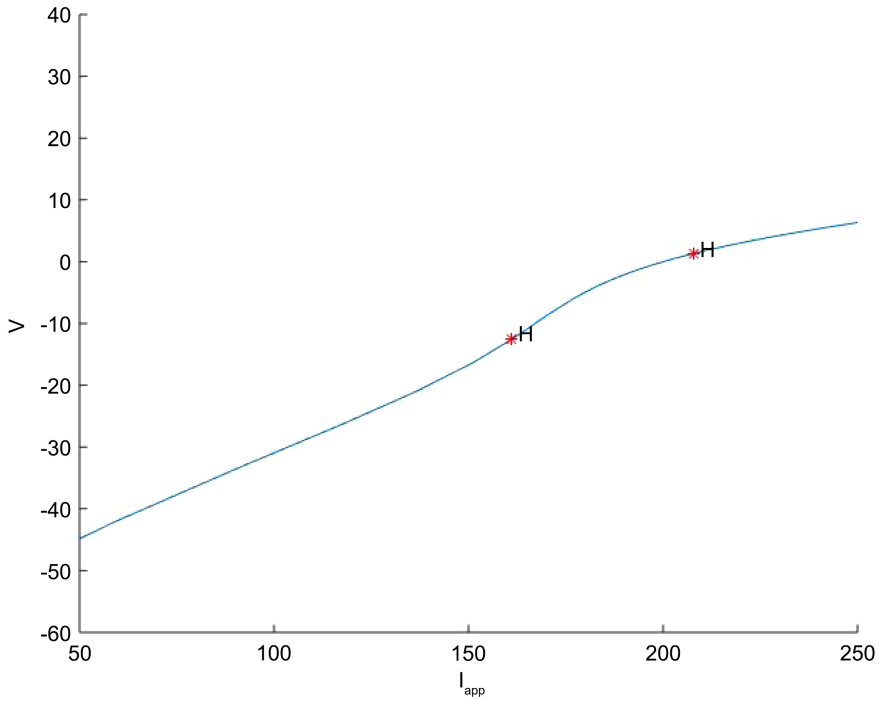


Figure 6. Continuation of equilibrium points in model (1) with the parameters similar to the Hopf case in Table 1.

Thus, there should exist an unstable limit cycle, bifurcating from the equilibrium and it indicates a subcritical Hopf Bifurcation for the first point and for the second point we have supercritical Hopf bifurcation a very small limit cycle is bifurcated at the bifurcation point. This limit cycle will grow with the further increasing of the injected current.

For the first point, the eigenvalues are $(\lambda_1, \lambda_2) = (2.70244e-08+i(0.176907), 2.70244e-08-i(0.176907))$. As we see, we have 2 complex conjugate eigenvalues with positive real part.

We can write the normal form for first Hopf point $(V, n) = (-12.596094, 0.274268)$ with the help of eigenvalues and the first Lyapunov coefficient as the form below

$$\dot{r} = (2.70244e-08)r + (8.624905e-05)r^3$$

$$\dot{\theta} = 0.176907$$

Here, $\dot{\theta} > 0$ as we know $\theta$ is the angle of oscillations that here is positive and increasing because the frequency of damped or sustained oscillations around this point $\omega_0$, is positive. But for the following normal form

$$\dot{r} = (2.70244e-08)r + (8.624905e-05)r^3$$

$$\dot{\theta} = -0.176907$$

Here, $\dot{\theta} < 0$ as we know $\theta$ is the angle of oscillations that here is negative and decreasing because the frequency of damped or sustained oscillations around this point $\omega_0$, is negative.

However, the analysis of normal form is just limited to the first equation of normal form.

$$\begin{aligned} &(2.70244e-08)r+(8.624905e-05)r^3=0\\ &\rightarrow \quad r\left((2.70244e-08)+(8.624905e-05)r^2\right)=0 \end{aligned}$$

So

$$r=0,\quad (2.70244e-08)+(8.624905e-05)r^2=0$$

Here, $r=0$ is an equilibrium and because for $r=0$

$$\frac{\mathrm{d}}{\mathrm{d}r}\left[(2.70244e-08)r+(8.624905e-05)r^3\right]=(2.70244e-08)>0$$

As a result, this equilibrium is unstable. The equation $(2.70244e-08)+(8.624905e-05)r^2=0$ does not give us any periodic solutions or oscillatory behaviors.

For other Hopf point with the eigenvalues $(\lambda_1,\lambda_2)=(-2.39388e-07+i(0.282179),-2.39388e-07-i(0.282179))$ we have the following normal form (for $(V,n)=(1.318376,0.488642)$)

$$\dot{r}=(-2.39388e-07)r-(-2.972401e-04)r^3$$

$$\dot{\theta}=0.282179$$

Here, $\dot{\theta}>0$ like above we know $\theta$ is the phase of oscillations that here is positive and increasing because the frequency of damped or sustained oscillations around this point, $\omega_0$, is positive. But for the following normal form

$$\dot{r}=(-2.39388e-07)r-(-2.972401e-04)r^3$$

$$\dot{\theta}=-0.282179$$

$\dot{\theta}<0$ as we know $\theta$ is the angle of oscillations that here it is negative and decreasing because the frequency of damped or sustained oscillations around this point $\omega_0$, is negative.

But, we know that the analysis of normal form depends on the first equation of normal form

$$\begin{aligned} &(-2.39388-07)r-(-2.972401e-04)r^3=0\\ &\rightarrow \quad r\left((-2.39388e-07)-(-2.972401e-04)r^2\right)=0 \end{aligned}$$

Therefore

$$r=0,\quad (-2.39388e-07)-(-2.972401e-04)r^2=0$$

Here, $r=0$ is an equilibrium and because for $r=0$

$$\frac{\mathrm{d}}{\mathrm{d}r}\left[(-2.39388e-07)r-(-2.972401e-04)r^3\right]=(-2.39388e-07)<0$$

As a result, this equilibrium is stable. The equation $(-2.39388e-07)-(-2.972401e-04)r^2=0$ gives us the stable periodic solution with amplitude

$$r = \sqrt{\frac{2.39388e-07}{2.972401e-04}}$$

### 3.1. $g_{inh}$ as Bifurcation Parameter

In this section, we consider $g_{inh}$ and $I_{app}$ as free parameters.

If we continue to increase $I_{app}$, the period of limit cycle becomes 2-times and then $2^2$ and … Here we say that the system undergoes the period-doubling bifurcation. As we do continuation of Hopf point, the trajectory repeats itself while we passed through *PD* point and we can see the trajectory is going around the loop twice before coming back to *PD* point. For period-doubling bifurcation a new limit cycle creates from the primary limit cycle, and the period of this new limit cycle is two times the previous limit cycle (see Figure 7 and Figure 8).

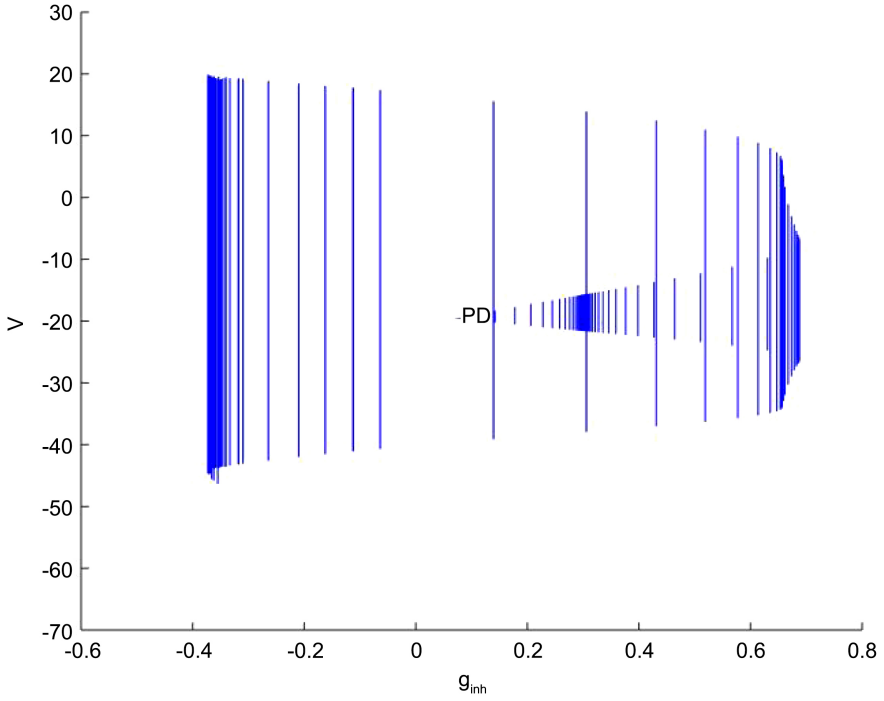


Figure 7. Continuation of period-doubling bifurcation from supercritical Hopf bifurcation.

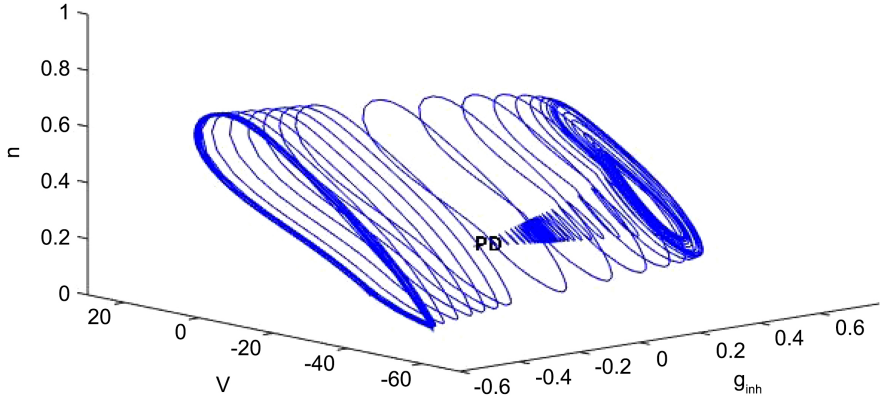


Figure 8. Computed limit cycle curve started from a period-doubling bifurcation.

If we increase $I_{app}$ further, the limit cycle that is born from supercritical Hopf bifurcation undergoes another period-doubling bifurcation. The Period-doubling can continue to infinity. But, in this procedure, the values of $I_{app}$ at which this bifurcation occurs become closer than before.

For localization of Branch Points of cycles, a special algorithm which is of Newton type Continuation Method has been used to show these singularities. Also, the equilibrium curve can have two generic codimension one bifurcation limit point and Hopf point and plus continuation of equilibrium curve gives us Branch Point that in Figure 9, Figure 10, it has been shown by *BPC*.

The branch point $Z_0$ for the complex valued function $f(z)$, has this property that the value of $f(z)$ does not return to its initial value as a closed curve around a point is traced, in such a way that $f$ varies continuously as the pass is traced.

Moreover, In the contex of complex analysis, a branch point of a multi-valued function is a point at which the function is discontinuous when it is going in a neighborhood of this point.

If we only consider $g_{inh}$ as bifurcation parameter, we have

label = $H$, $x = (-19.573692 \quad 0.191817 \quad 0.071067)$
Neutral saddle

label = $LP$, $x = (-4.616109 \quad 0.391485 \quad 0.187732)$
$a = 8.199830e-03$

label = $H$, $x = (6.041592 \quad 0.566955 \quad -0.192795)$
First Lyapunov coefficient = 7.969763e−04

In this case, we have a natural saddle in $(V, n) = (-19.573692, 0.191817)$ and $g_{inh} = 0.071067$ for which $\lambda_1 + \lambda_2 = 0$.

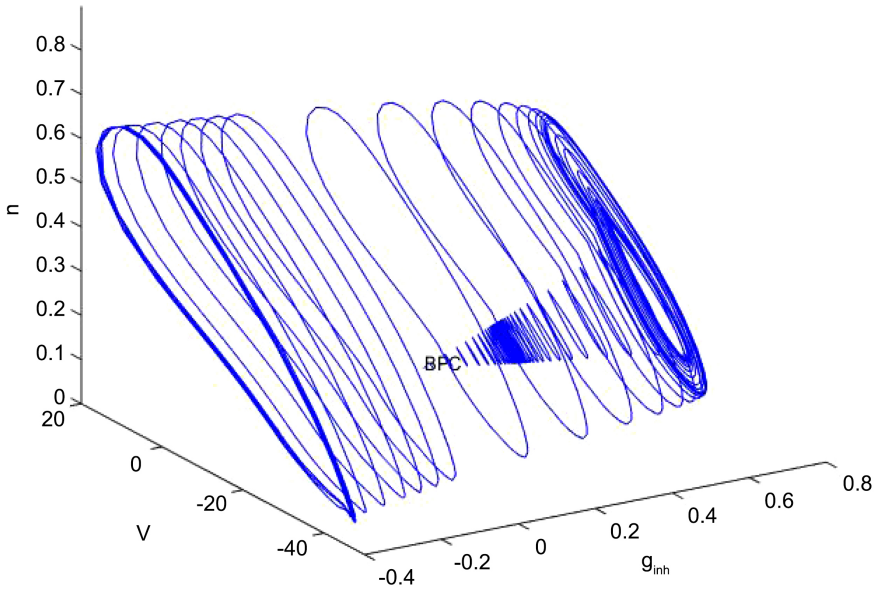


Figure 9. Continuation of branch point cycles from equilibrium curve.

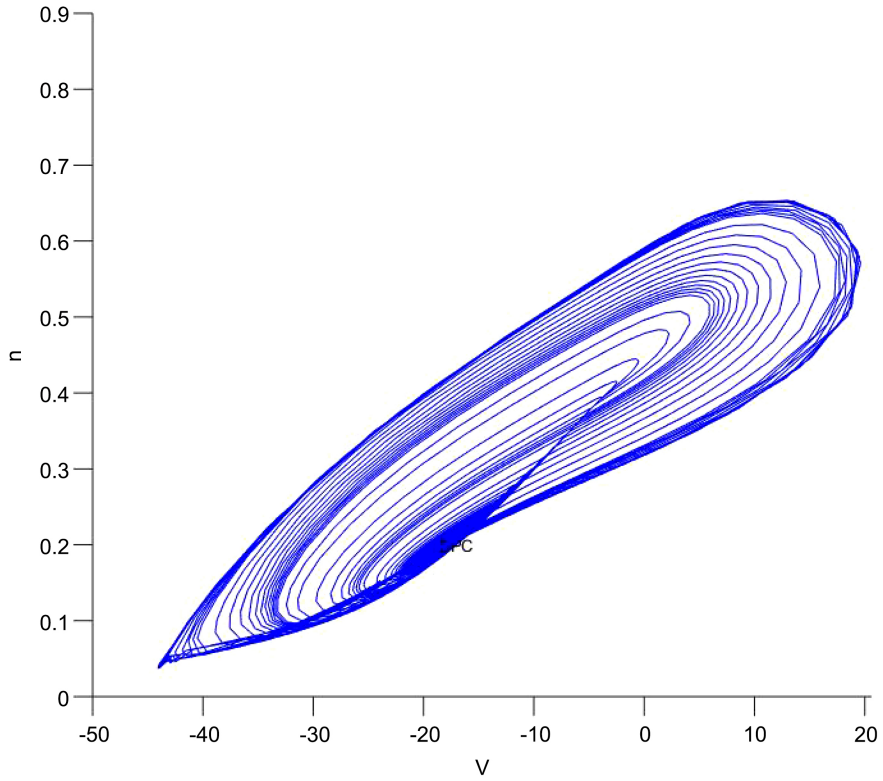


**Figure 10.** Continuation of branch point cycles from equilibrium curve.

Also for $(V,n)=(6.041592,0.566955)$ and $g_{inh}=-0.192795$ and for the eigenvalues $(\lambda_1,\lambda_2)=(-1.75069e-07+i(0.291426),-1.75069e-07-i(0.291426))$ we have a subcritical Hopf bifurcation with the following normal form

$$\dot{r}=(-1.75069e-07)r+(7.969763e-04)r^3$$

$$\dot{\theta}=0.291426$$

Here, $\dot{\theta}>0$ as we know $\theta$ is the angle of oscillations that here is positive and increasing because the frequency of damped or sustained oscillations around this point $\omega_0$, is positive. But for the following normal form

$$\dot{r}=(-1.75069e-07)r+(7.969763e-04)r^3$$

$$\dot{\theta}=-0.291426$$

Here, $\dot{\theta}<0$ as we know $\theta$ is the angle of oscillations that here is negative and decreasing because the frequency of damped or sustained oscillations around this point $\omega_0$, is negative.

However, the analysis of normal form is just limited to the first equation of normal form.

$$(-1.75069e-07)r+(7.969763e-04)r^3=0$$

$$\rightarrow \quad r\left((-1.75069e-07)+(7.969763e-04)r^2\right)=0$$

So

$$r=0,\quad (-1.75069e-07)+(7.969763e-04)r^2=0$$

Here, $r=0$ is an equilibrium and because for $r=0$

$$\frac{\mathrm{d}}{\mathrm{d}r}\left[\left(-1.75069e-07\right)r+\left(7.969763e-04\right)r^3\right]=\left(-1.75069e-07\right)<0$$

As a result, this equilibrium is stable. The equation $\left(-1.75069e-07\right)+\left(7.969763e-04\right)r^2=0$ gives us the stable periodic solution with amplitude

$$r=\sqrt{\frac{1.75069e-07}{7.969763e-04}}$$

The complete bifurcation diagram with respect to $g_{inh}$ has been demonstrated in Figure 11.

In Figure 11, codimension two bifurcations Bogdanov-Takens and Cusp bifurcations have been demonstrated. Bogdanov-Takens bifurcation is a codimension two bifurcation that has the following normal form

$$\dot{u}=v$$

$$\dot{v}=a+bu+u^2+\sigma uv$$

where, $a,b$ are the normal form coefficients, and the parameter $\sigma=1,-1$ depends on different types of supercritical and subcritical.

In another word, when cusp bifurcation happens, we have a Saddle-Node bifurcation at an equilibrium point, when for the system $\dot{x}=f\left(x,\gamma\right)$ we have $f_x=0$ and $f_{xx}\neq 0$ and this system is equivalent with $\dot{x}=a\left(\gamma\right)+x^2$.

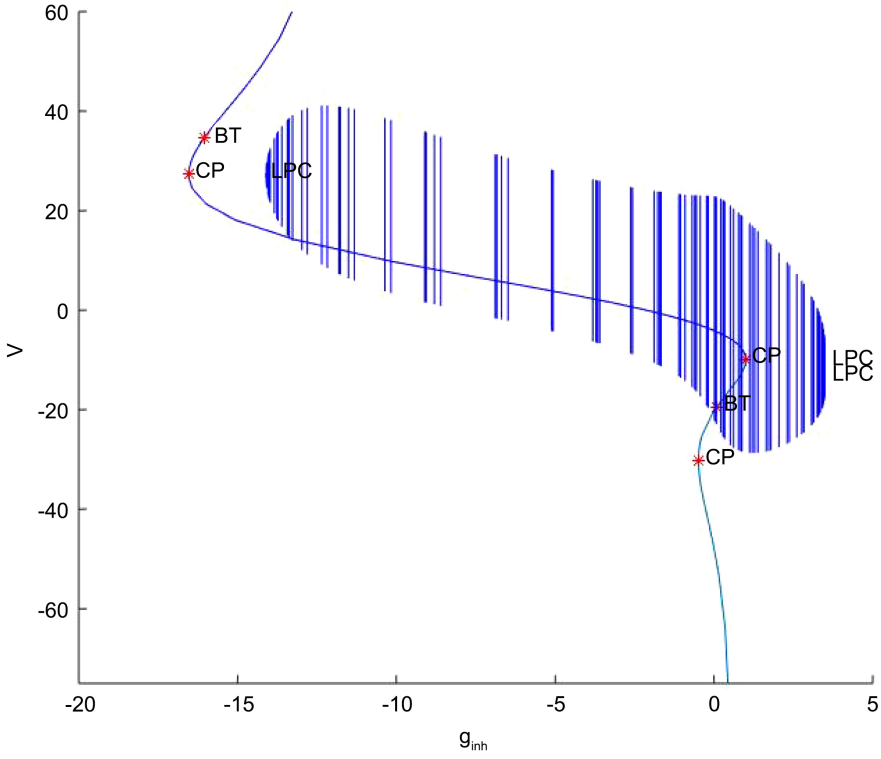


Figure 11. Complete bifurcation continuation.

When we have $f_{xx}=0$ and $f_{xxx}\neq 0$, then the equilibrium point undergoes cusp bifurcation that is a codimension two bifurcation with respect to $I_{app}, g_{inh}$ as bifurcation parameters. The system near the cusp point obeys the following normal form

$$\dot{x}=a_1(\gamma)+a_2(\gamma)x+cx^3$$

So that

$$a_1(\gamma)=f(x_\gamma,\gamma),\quad a_2(\gamma)=f_x(x_\gamma,\gamma),\quad c=f_{xxx}/6\neq 0$$

If $c>0$ we have subcritical cusp bifurcation and if $c<0$, we have supercritical cusp bifurcation. To find the bifurcation set:

$$\frac{\mathrm{d}}{\mathrm{d}x}\left(a_1(\gamma)+a_2(\gamma)x+cx^3\right)=a_2(\gamma)+3cx^2=0$$

which gives the following saddle-node curves

$$a_1(\gamma)=+\frac{2}{\sqrt{a}}\left(\frac{a_2(\gamma)}{3}\right)^{3/2},\quad a_2(\gamma)=-\frac{2}{\sqrt{a}}\left(\frac{a_2(\gamma)}{3}\right)^{3/2}$$

Also, we know that if $a_1(\gamma)=0$ and $a_2(\gamma)=\gamma$, we have the following normal form

$$\dot{x}=\gamma x+cx^3$$

which is the normal form for Pitchfork bifurcation.

Here, for the first point

label = *CP*, $x=(-10.008656\quad 0.309902\quad 221.927487\quad 0.996196)$
$c=5.411489e-04$

$$\left(a_1(\gamma),a_2(\gamma)\right)=\left(I_{app},g_{inh}\right)=(221.927487,0.996196)$$

So that we can easily write the normal form for this equilibrium point and we can find the bifurcation set and saddle-node curves.

### 3.2. $g_{exc}$ as Bifurcation Parameter

In this section, we consider $g_{exc}$ and $I_{app}$ as free parameters.

At first, we assume $g_{exc}$ as bifurcation parameter (see Figure 12).

In Figure 12 we have:

label = *H*, $x=(-7.210500\quad 0.351140\quad 1.975854)$
First Lyapunov coefficient = −9.396562e−04

label = *H*, $x=(-12.596098\quad 0.274268\quad 0.209999)$
First Lyapunov coefficient = 8.625008e−05

For the first Hopf point $(V,n)=(-7.210500,0.351140)$ and $g_{exc}=1.975854$ and the eigenvalues $(\lambda_1,\lambda_2)=(-3.66907e-08+i(0.232446),-3.66907e-08-i(0.232446))$ we have a supercritical Hopf bifurcation with the following normal form

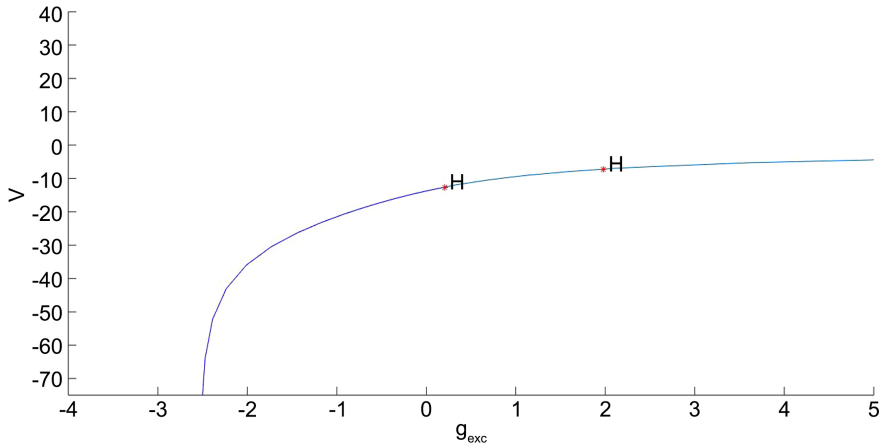


**Figure 12.** $g_{exc}$ as free parameter, continuation of Hopf points.

$$\dot{r} = (-3.66907e-08)r - (-9.396562e-04)r^3$$

$$\dot{\theta} = 0.232446$$

Here, $\dot{\theta} > 0$ as we know $\theta$ is the angle of oscillations that here is positive and increasing because the frequency of damped or sustained oscillations around this point $\omega_0$, is positive. But for the following normal form

$$\dot{r} = (-3.66907e-08)r - (-9.396562e-04)r^3$$

$$\dot{\theta} = -0.232446$$

Here, $\dot{\theta} < 0$ as we know $\theta$ is the angle of oscillations that here is negative and decreasing because the frequency of damped or sustained oscillations around this point $\omega_0$, is negative.

However, the analysis of normal form is just limited to the first equation of normal form.

$$(-3.66907e-08)r - (-9.396562e-04)r^3 = 0$$
$$\rightarrow r\left((-3.66907e-08) - (-9.396562e-04)r^2\right) = 0$$

So

$$r = 0, \quad (-3.66907e-08) - (-9.396562e-04)r^2 = 0$$

Here, $r = 0$ is an equilibrium and because for $r = 0$

$$\frac{\mathrm{d}}{\mathrm{d}r}\left[(-3.66907e-08)r - (-9.396562e-04)r^3\right] = (-3.66907e-08) < 0$$

As a result, this equilibrium is stable. The equation $(-3.66907e-08) - (-9.396562e-04)r^2 = 0$ gives us the stable periodic solution with amplitude

$$r = \sqrt{\frac{3.66907e-08}{9.396562e-04}}$$

For other Hopf point with the eigenvalues $(\lambda_1, \lambda_2) = (2.6594e-11 + i(0.176907), 2.6594e-11 + i(0.176907))$ we have the

following normal form (for $(V,n)=(-12.596098,0.274268)$ and $g_{exc}=0.209999$ )

$$\dot{r}=(2.6594e-11)r+(8.625008e-05)r^3$$

$$\dot{\theta}=0.176907$$

Here, $\dot{\theta}>0$ like above we know $\theta$ is the phase of oscillations that here is positive and increasing because the frequency of damped or sustained oscillations around this point, $\omega_0$, is positive. But for the following normal form

$$\dot{r}=(2.6594e-11)r+(8.625008e-05)r^3$$

$$\dot{\theta}=-0.176907$$

$\dot{\theta}<0$ as we know $\theta$ is the angle of oscillations that here it is negative and decreasing because the frequency of damped or sustained oscillations around this point $\omega_0$, is negative.

But, we know that the analysis of normal form depends on the first equation of normal form

$$(2.6594e-11)r+(8.625008e-05)r^3=0$$
$$\rightarrow r\left((2.6594e-11)+(8.625008e-05)r^2\right)=0$$

Therefore

$$r=0,\quad (2.6594e-11)+(8.625008e-05)r^2=0$$

Here, $r=0$ is an equilibrium and because for $r=0$

$$\frac{\mathrm{d}}{\mathrm{d}r}\left[(2.6594e-11)r+(8.625008e-05)r^3\right]=(2.6594e-11)>0$$

As a result, this equilibrium is unstable. The equation $(2.6594e-11)+(8.625008e-05)r^2=0$ does not give us the periodic solutions.

Also, at $g_{inh}=0.071067341$ and considering $g_{exc}$ as bifurcation, parameter with changing the period we have the result in Figure 13 and Figure 14.

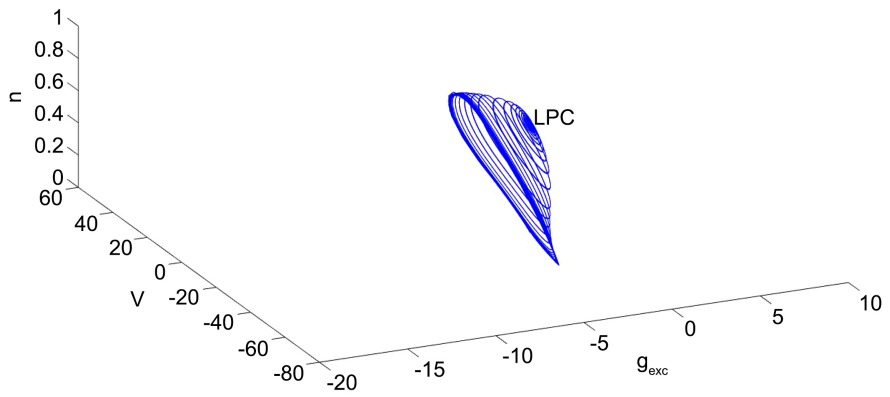


Figure 13. $g_{exc}$ as free parameter, computed limit cycle curve started from a Hopf bifurcation.

## 4. The Homoclinic Case

In this section, we study the homoclinic bifurcation using the parameter values from Table 1.

When a saddle homoclinic bifurcation occurs a limit cycle disappears or born. A saddle point has two stable and unstable submanifolds. When we change the parameters for bifurcation, these two submanifolds collide and create one homoclinic orbit as we see clearly in Figure 15. After and before the moment of bifurcation we do not have this homoclinic orbit.

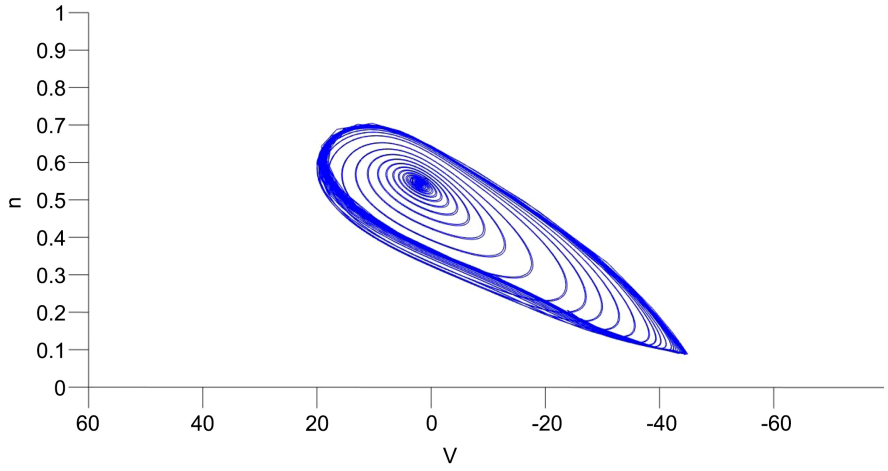


Figure 14. $g_{exc}$ as free parameter, Continuation of limit point cycle from Hopf point in $(V,n)$ -plane.

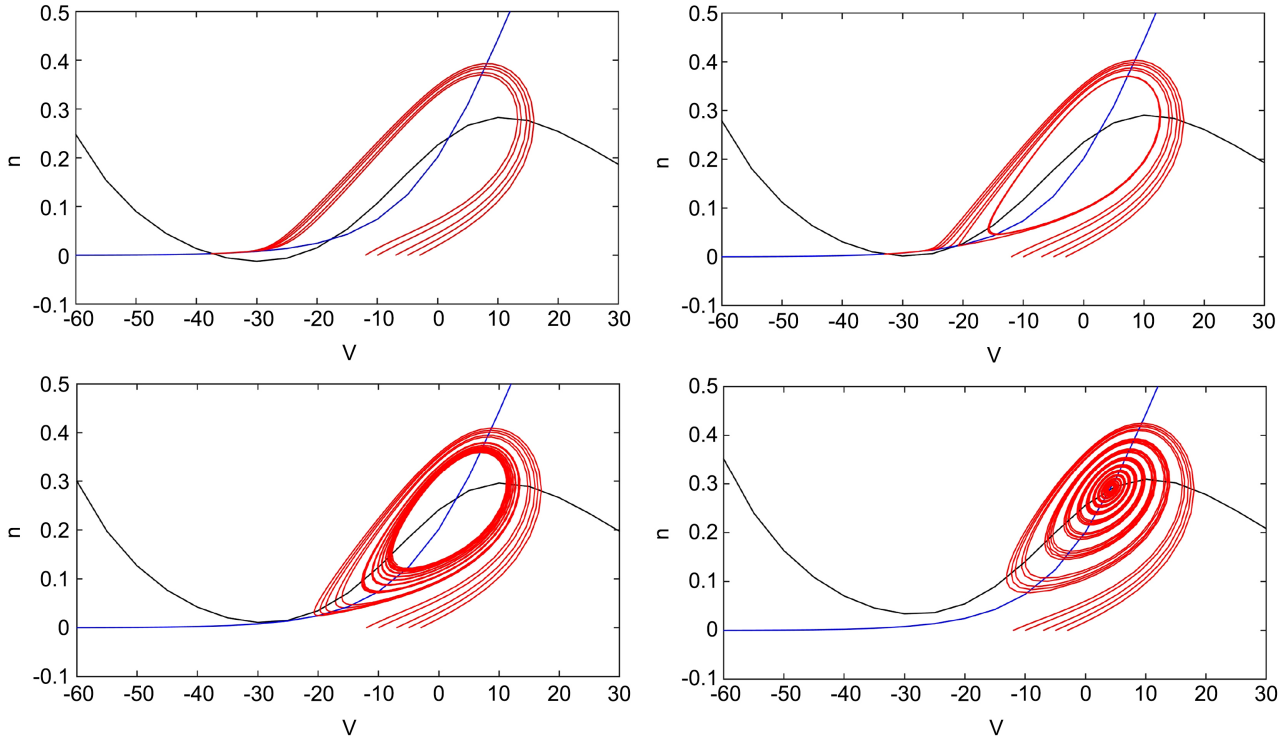


Figure 15. Saddle homoclinic bifurcation. $I_{app} = 40$ (up, left), $I_{app} = 46$ (up, right), $I_{app} = 50$ (down, left), $I_{app} = 60$ (down, right).

In neuroscience point of view, before the beginning of bifurcation, all trajectories go back to the resting state after a counter-clockwise excursion (firing spike) and we have limit cycle attractors corresponding to periodic spiking. At the moment of bifurcation, we have periodic spiking activity with the period that goes to infinity (the period of limit cycle goes to infinity). After the bifurcation the state of the system again goes back to the rest and we do not have tonic spiking.

There is another bifurcation similar to saddle Homoclinic bifurcation and in both of them we have a Homoclinic orbit that begins and finishes in the same equilibrium point. But saddle-Homoclinic is of codimension 1 and saddle-node Homoclinic is of codimension two. For saddle-node Homoclinic we must have the condition for occurrence of saddle-node bifurcation $\lambda_1 = 0$ and also the saddle-node quantity $\lambda_1 + \lambda_2 < 0$ it means that $\lambda_2 < 0$. As a result, in saddle-node Homoclinic, we observe the appearance or disappearance of a stable limit cycle.

## 5. Discussion and Conclusion

In this study we discovered the biological and spiking behaviors of Morris-Lecal neuron model including a new more channel, chloride channel, and we compared it to the original model. Morris-Lecal neuron model with two ordinary differential equations is a reduction version of Hodgkin-Huxley model. We have shown that for different biological parameters values, the model displays quiescent and spiking behaviors. To explore the exciting behaviors of neuron, we conducted different numerical simulations and bifurcation analysis. We obtained numerically the Hopf bifurcation and homocinic bifurcation at larger values for injected current compared to the original model and we derived them analytically by finding their normal forms. Specifically, we conducted rigorous bifurcation analysis and continuation of equilibrium point with respect to the injected current or changing other biological parameters and we explored the complicated and interesting dynamics of new Morris-Lecar model such as different fluctuations neuronal patterns.

In supercritical Hopf bifurcation, when we changed the control parameters (bifurcation parameters), we could see a stable equilibrium point lost its stability and a stable limit cycle bifurcated from it. In this case, the state of the system stayed near the equilibrium and we could see only small amplitude oscillations around the equilibrium point. When we changed the parameter in the opposite direction the limit cycle degenerated to a point and we reached the previous equilibrium point. We noticed that as it is expected this neuron that has undertaken supercritical Hopf bifurcations did not show an immediate spike and it remained quiescent (it displayed small amplitude sustained oscillations).

In other cases, for subcritical Hopf bifurcation, when we changed the bifurcation parameter, we noticed the immediate spike or a large amplitude jump in time series of system equations. In this case, when we changed the parameter in

opposite direction, the equilibrium became stable again but the state of the system went back to its similar saddle-node bifurcation or saddle-Homoclinic bifurcations.

As we have seen for model (1), there are different types of codimension-two bifurcations which occurred when we had two bifurcation parameters. One of them was the Bogdanov-Takens bifurcation which is a codimension-two bifurcation of an equilibrium point in a two-dimensional system for which the equilibrium point has two zero eigenvalues. Near the bifurcation parameter, we have two equilibrium points, a saddle point and others that are not a saddle point which collides and disappears via a saddle-node bifurcation. For the equilibrium that was not saddle, we have seen Hopf bifurcation that produced a limit cycle. This single limit cycle degenerated to a Homoclinic orbit to the saddle and disappeared via a saddle homoclinic bifurcation. Bogdanov-Takens bifurcation can occur when an equilibrium undergoes Hopf bifurcation and saddle-node bifurcation simultaneously and also it occurs when we have two-dimensional systems. Therefore, for this model we showed that we have a transition between integrator and resonator as the neuron that undergoes saddle-node bifurcation is an integrator (without damped subthreshold oscillations) and the neuron that undergoes Hopf bifurcation is a resonator (with damped subthreshold oscillations).

Continuation of limit cycles from the Hopf point, gave us the limit point (Fold/Saddle Node) bifurcation. Limit point cycles are a set of limit cycles that bifurcate from the Hopf point, and moreover, limit point cycle (LPC) is a fold bifurcation for which two limit cycles with different periods are near the LPC point. Likewise, as we saw, the continuation of cycles from a Hopf point also gave period doubling (flip) bifurcations. Period doubling bifurcation is a bifurcation for which a new limit cycle creates from the limit cycle that exists and the period of the new limit cycle is twice the first limit cycle. Moreover, we have shown changing the type of Hopf bifurcation from supercritical to subcritical which means that the type of stability changes from monostability in supercritical to bistability in subcritical Hopf bifurcation.

## Conflicts of Interest

The authors declare no conflicts of interest regarding the publication of this paper.

## References

[1] Izhikevich, E.M. (2007) Dynamical Systems in Neuroscience. MIT Press, Cambridge. https://doi.org/10.7551/mitpress/2526.001.0001

[2] Izhikevich, E.M. (2003) Simple Model of Spiking Neurons. *IEEE Transactions on Neural Networks*, **14**, 11569-1572. https://doi.org/10.1109/TNN.2003.820440

[3] Izhikevich, E.M. (2004) Which Model to Use for Cortical Spiking Neurons? *IEEE Transactions on Neural Networks*, **15**, 1063-1070. https://doi.org/10.1109/TNN.2004.832719

[4] Izhikevich, E.M. (2000) Neural Excitability, Spiking and Bursting. *International*

*Journal of Bifurcation and Chaos*, **10**, 1171-1266.
https://doi.org/10.1142/S0218127400000840

[5] Cai, R., Liu, Y.C., Duan, J.Q. and Abebe, A.T. (2020) State Transitions in the Morris-Lecar Model under Stable Lévy Noise. *The European Physical Journal B*, **93**, 1-9. https://doi.org/10.1140/epjb/e2020-100422-2

[6] Rinzel, J. and Ermentrout, G.B. (1989) Analysis of Neural Excitability and Oscillations. MIT Press, Cambridge.

[7] Ermentrout, G.B. and Terman, D.H. (2010) Mathematical Foundations of Neuroscience. Springer Science & Business Media, Berlin, 35. https://doi.org/10.1007/978-0-387-87708-2

[8] Ermentrout, B. (1996) Type I Membranes, Phase Resetting Curves, and Synchrony. *Neural Computation*, **8**, 979-1001. https://doi.org/10.1162/neco.1996.8.5.979

[9] Hodgkin, A.L. and Huxley, A.F. (1952) A Quantitative Description of Membrane Current and Its Application to Conduction and Excitation in Nerve. *The Journal of Physiology*, **117**, 500-544. https://doi.org/10.1113/jphysiol.1952.sp004764

[10] Hodgkin, A.L. (1948) The Local Electric Changes Associated with Repetitive Action in a Non-Medullated Axon. *The Journal of Physiology*, **107**, 165-181. https://doi.org/10.1113/jphysiol.1948.sp004260

[11] Morris, C. and Lecar, H. (1981) Voltage Oscillations in the Barnacle Giant Muscle Fiber. *Biophysical Journal*, **35**, 193-213. https://doi.org/10.1016/S0006-3495(81)84782-0

[12] Azizi, T. and Mugabi, R. (2020) The Phenomenon of Neural Bursting and Spiking in Neurons: Morris-Lecar Model. *Applied Mathematics*, **11**, 203-226. https://doi.org/10.4236/am.2020.113017

[13] FitzHugh, R. (1961) Impulses and Physiological States in Theoretical Models of Nerve Membrane. *Biophysical Journal*, **1**, 445-466. https://doi.org/10.1016/S0006-3495(61)86902-6

[14] Kuznetsov, Y.A. (2013) Elements of Applied Bifurcation Theory. Springer Science & Business Media, Berlin, 112.

[15] Wiggins, S. (2003) Introduction to Applied Nonlinear Dynamical Systems and Chaos. Springer Science & Business Media, Berlin, 2.